

Dynamic susceptibility induced asymmetry of MR proton resonance frequency (PRF) thermometry maps during simultaneous RF ablation causing large and spatially dependent temperature errors

M. Viallon¹, E. Dumont², J. Roland³, C. D. Becker¹, S. Terraz¹, and R. Salomir¹

¹Radiology, Geneva University Hospital, Geneva, Switzerland, ²Image Guided Therapy, PESSAC, France, ³R & D, Siemens Medical Solutions, Erlangen, Germany

Introduction

MR thermometry based on the proton resonance frequency (PRF) method (1) has gained good acceptance for guiding RF ablation of liver tumors (2). Thermal dose model (TD) is a reliable predictor of cell death in thermal ablation technique (3). To derive a correct TD thus a correct cut-off point for the application of energy, temperature evolution has to be accurately measured throughout the treatment. Previous works focused on proving the accuracy of MR thermometry with the PRF method: ex-vivo using optical temperature probes to provide reference temperature measurements during simultaneous RF ablation or in animals (4) after in-vivo procedure by comparison of the effectively coagulated lesion size defined by histopathology and the measured TD size (5). None of these experiment reported spatially related errors in temperature maps and TD during power application, while using single slice 2D experimental imaging setup. We described here dynamic susceptibility induced 3D asymmetry effect causing errors in the TD estimates.

Materials and Methods

A bipolar internally-cooled electrode was inserted in a homogeneous sample of fresh pork muscle. The experiment was repeated twice: once with the RF electrode positioned along the Bo field to minimize the susceptibility artifact of the needle, and second orthogonally to Bo to maximize the susceptibility effect. RF power (15W, duration of heating 166 s, energy of 2.5 kJ) was applied simultaneously to the MR imaging with an RF generator (Celon AG, Teltow, Germany) working at 475 kHz. The generator was placed outside the Faraday cage, and the transmission line traversed a wave guide of the cage. Three low pass LC stopband filters ($f_0 = 63.5$ MHz) and 6 ferrite cores were added to the transmission line to provide an 80dB attenuation of harmonic at the resonant frequency. A low power setting was chosen to minimize disrupting effects such as vaporization along the muscle fibers (4KJ over 160sec i.e. 25W/35W average/peak power). The sample was imaged on a 1.5T MR system (Espree, Siemens AG, Germany). 3 orthogonal slices were chosen: a transverse plane orthogonal to the RF electrode and cutting it midway between its anode and cathode active zones, and both a sagittal and coronal plane parallel to the electrode. All were determined from a high resolution T1 3D gradient-echo (Vibe) acquisition. A dynamic series of 60 magnitude and phase images was acquired using an rf-spoiled gradient echo sequence with fat saturation in these 3-plane locations during the power application (10 dynamics were acquired prior to the onset of RF power, dynamics 11-20, 26-35 and 41-50 during power application, dynamic 21-25, 36-40 and 51-60 pausing power application). Main Imaging parameters were: slices = 3, dynamics = 60, acquisition time/dynamic = 2.55s (total imaging time was 178.5 s) repeated every 5 sec (simulated respiratory cycle), voxel = $1.6 \times 1.6 \times 6.0$ mm, matrix = 128×128 , TR/TE/FA = 200/17/25, coils = flex loop, 3 spine arrays, coil mode = auto (CP). Images were sent in real-time to a post-processing software (ThermoGuide, Image Guided Therapy, Pessac, France) that applied phase unwrapping and calculated the relative temperature rise at each pixel (2), including a temperature baseline drift correction.

Results

Temperature maps (figure 1) and Magnitude images with the electrode susceptibility artifact (figure 2) are shown for two power settings (during and between RF power application) and for the two experimental situations (parallel and perpendicular to Bo). T° over time (derived in one pixel identified with a red cross) is displayed in figure 3, and clearly indicate artifactual T° drop during power application.

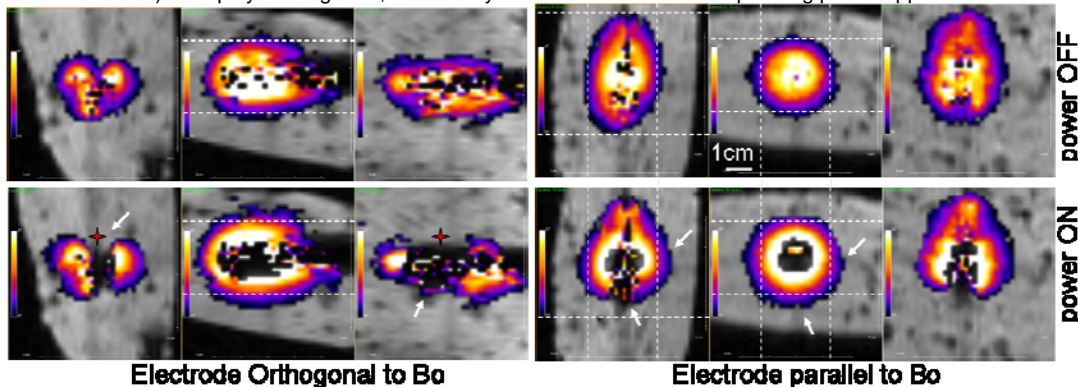


Figure 1. Magnitude image and calculated Tmap superimposed obtained when the needle is orthogonal (left) and parallel (right) to Bo and during power application (bottom) and after cutting it off (top). Temperature levels increase from blue (37°C) to white (65°C and above) for a qualitative appreciation of the shape of the heating pattern. During heating, the expected isothermal surface is a 3D ellipsoid with the long axis coinciding with the axis of the RF electrode (Top left images). Bottom images show that the temperature pattern change from the symmetric expected 3D ellipsoid pattern to a pattern varying depending on the orientation between the electrode and Bo, suggesting susceptibility change over time and/or T° .

Discussion and Conclusion

The direction of the effect (apparent T° increase/decrease is dependent on the slice orientation and electrode orientation and can cause either overestimation (worst case) or underestimation of the thermal dose. This artifact in the temperature maps is likely to be caused by gas bubbles forming during heating, which can be approximated as a spherical object with a different susceptibility compared to tissue and causing a recognizable dipole magnetic field disturbance. Control experiment with passive electrode in water bath at 20°C and 90°C confirms that the observed effects cannot be attributed to odd needle susceptibility changes with temperature. For future in-vivo studies, the MR method will require correction of the thermal dose estimate for this effect, since such inaccuracy will prevent using the actual TD for treatment cut-off. Further theoretical analysis and simultaneous experimental comparison with optical temperature probes are needed to solve this problem in order to reliably base clinical procedure end point on TD estimates.

References: (1) Ishihara Y et al. MRM 1995;34(6):814-823. (2) Quesson B et al. JMIR 2000;12(4):525-533. (3) Seror O et al. Eur Radiol.2008;18(2):408-16. (4) Cernicanu et al. NMR Biomed.2008; 21(8):849-58. (5) Lepetit-coiffé M et al. JMIR 2006; 24:152-159.

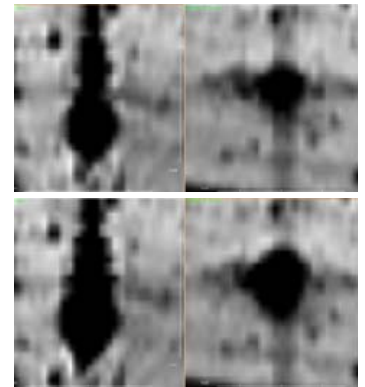


Figure 2. Electrode susceptibility artifact during (bottom) and between (Top) RF power applications. On the magnitude images, the artifact appearance changes and its size is increased.

Figure 3. Temperature curve over time obtained in one point (red cross) in figure 1 with electrode perpendicular to Bo. Temperature is apparently diminishing during power application and recovering during pause of power application. The reproducible T° disturbance disappear when setting off power application (in the order of 10°C) and the temperature maps returned systematically to a more regular appearance (upper case).

